UNIVERSITY OF MISKOLC

FACULTY OF MECHANICAL ENGINEERING AND INFORMATICS

Increase the efficiency of the hybrid photovoltaic thermal system

Booklet of PHD dissertation

PREPARED BY:

Mohammed Alktranee

ISTVÁN SÁLYI DOCTORAL SCHOOL OF MECHANICAL ENGINEERING SCIENCES

MAIN TOPIC GROUP: FUNDAMENTAL SCIENCES IN MECHANICAL ENGINEERING

TOPIC GROUP: TRANSPORT PROCESSES AND MACHINES

Head of Doctoral School
Bognár Vadászné Gabriella
Director of Science, Full Professor

Scientific Supervisor

Bencs Péter
Associate professor

Miskolc
2023

JUDGING COMMITTEE

chair:

secretary:

members:

OFFICIAL REVIEWERS

1. Introduction

Modern economies mainly depend on long-term energy availability for future economic growth. The energy sector has manifested significant concerns due to the unavailability of sufficient energy resources and increasing conventional energy demands due to human activities [1]. In recent decades, renewable energy sources have developed rapidly, reaching significant usage percentages in several countries, particularly for electricity supply [2]. Solar energy systems that convert sunlight into heat or electricity are one of the most important technologies of renewable energy systems and a better alternative for environmental safety since they rely on solar energy, which is freely available and most sustainable in the future [3]. Photovoltaic (PV) is amongst solar energy technologies that consist of semiconductor materials and work to convert sunlight (i.e. short-wavelength energy) to electricity [4]. Given that PV modules work outdoors, they are constantly affected by weather conditions, such as temperature, solar radiation and wind [5]. Generally, PV modules convert below 20% of solar radiation into electricity, and the remainder is converted into heat, causing long-term and short-term problems for PV modules. Environmental factors, such as ultraviolet intensity, temperature and water, ingress into PV cells and cause performance degradation of PV modules (i.e. long-term problem). Meanwhile, increasing PV cell temperature negatively affects cell conversion efficiency, decreasing the PV module's electrical power yield (i.e. short-term problem) [6]. Increasing PV cell temperature drops open-circuit voltage and 0.4–0.5% in PV cell efficiency compared with the standard test condition STC (1000 W/m^2 and 25 °C) [7]. Thus, the reliability and lifetime of PV modules are affected [8]. Different cooling techniques help reduce productivity losses and enhance PV module efficiency at high temperatures. Passive and active cooling techniques have been commonly used to maintain PV module performance at high operating temperatures. Passive cooling does not require external power for cooling the PV module, whereas active cooling needs it.

2. Objectives

- This PhD dissertation addresses the uncompleted gaps in the literature that contributes to improving the general performance of the PVT system by adopting reliable technologies that contribute to improving PVT system performance. Energy and exergy analysis of the active and passive cooling is used to investigate their effect on the PV module's temperature reduction, electrical power generation, energy efficiency, exergy efficiency, exergy losses and entropy generation. Then comparing the results obtained with previous studies to develop a clear vision of using such techniques and economic analysis for the cooling techniques applied to show the feasibility of cooling techniques applied. Passive and active cooling was applied to decrease the temperature of the PV module and enhance its performance, as follows:
- A numerical simulation by ANSYS software to predict the thermal behaviour of the PV module at different operation conditions. Then testing, the outputs of the PV module depend on the mathematical equations to predict the electrical behaviour of the PV module by using the MATLAB-Simulink program.
- Investigate the effect of evaporating cooling generated by using cotton wicks immersed in water (CWIWs) as passive cooling.
- Experimental comparative study on using different cooling (passive and active) techniques with PV module.
- Effect of active cooling on energy and exergy of PVT system using new mono WO_3 and ZrO_2 nanofluids: An experimental study.

- The effect of cooling by modified mono nanofluids such as (TiO_2, CuO, and Fe_2O_3) nanofluids at different volume concentrations on the PVT system performance.
- The effects of new hybrid nanofluids consisting of TiO_2-CuO and TiO_2-Fe_2O_3 in the binary ratio of 50%:50% as a hybrid nanofluid at different volume concentrations on the energy, exergy, and entropy generation of the PVT system.
- A numerical simulation of the effect of mono and hybrid nanofluids as cooling fluids on PVT system performance.

3. Methodology

This chapter involves the system description, instruments used, and the scientific methodologies applied in the experimental measurements to accomplish the research objectives.

3.1 Experimental setup and procedure

3.1.1 Configuration of the passive cooling techniques

Cotton wicks (CWs) were attached with rectangular aluminium fins (RAFs) by thermal silicon and attached at the rear of the PV module by thermal silicon adhesive. Fins are used as a partial rectangle (52 cm long, 3 cm wide, and 1.5 mm thick) and uniform distance between RAFs. CWs were arranged in serpentine on the backside of the PV module, and fins formed contiguously without space between them. Table 1 shows the specifications of the CWIRAF components [22–24]. The CWs are characterized by a suitable heat transfer coefficient, lower thermal conductivity, and high absorbent capacity, which helps with the distribution of water to all CWs attached at the behind of the PV module without using extra power. In addition, it's locally available, cost-effective and does not require maintenance. A total of 11 CW ends were submerged at the bottom of three plastic bottles full of water to supply water to CWIRAFs during the experiment, as shown in Figure 1. The CW ends placed in the water tank continuously provided water from the top to the bottom of the PV module. Therefore, four thermocouples were placed on each of the surfaces of the PV modules at different places, three were placed on the backside, and one was used to measure ambient temperature. In the present study, solar radiation was measured manually for 30 min using a power meter (Type SM206) with a 0.1 W m^{-2} resolution. The temperature was measured through thermocouples installed at different PV module surfaces and backsides. Temperature, voltage and current were measured using an AT mega 2560 data logger multi-channel Arduino, which was programmed to record the data.

Table 1. Material specifications used for passive cooling

Rectangular fins		Cotton wick	
Material	Aluminum	Cotton wick diameter	8 mm
Number of fins	20	Cotton wick length	50 m
Thermal conductivity	237 W $m^{-1}K^{-1}$	Thermal conductivity	0.048 W $m^{-1}K^{-1}$
Specific heat	903 J $kg^{-1}K^{-1}$	Heat transfer coefficient	36 W m^{-1}°C^{-1}
Density	2702 kg m^{-3}	-	-

The data logger consisted of 17 thermocouples with 0.25 °C resolution for measuring temperature, two sensors to measure the voltage with a resolution of 0.02445 V and two current sensors. Table 2 shows the data logger specification. The data logger recorded data with 10 min time step throughout the experiment days and saved the data in portable storage memory of 8

GB. Two 18-V lamps were used to complete the electrical circuit between the PV module voltage and current sensors.

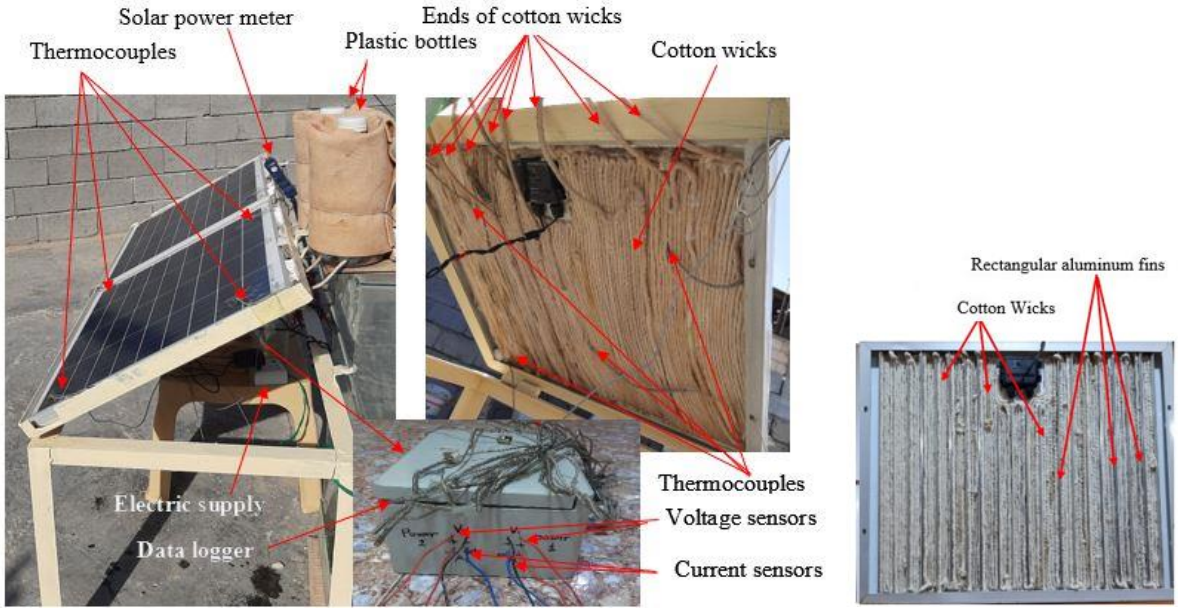

Figure 1. Configurations of PV with CWIWs and RAFs

Temperature and solar radiation are the operation parameters of the PV module work

Table 2. Specifications of devices/instruments used in the study

Item	Type/Model	Range	Accuracy
Thermocouples	K (2 m length)	−200 °C to 1350 °C	0.25 °C
Current sensor	ACS712	up to 30 A	0.04 A
Voltage sensor	Module 25V	up to 25 V	0.02445 V
Solar power meter	SM206	1-3999 W m^{-2}	±0.1W m^{-2}

3.1.2 Configuration of the active cooling techniques

Two polycrystalline PV modules of 50 W were used. The first PV module was left without cooling for referencing, whereas the second PV module was cooled with DI water and nanofluids. The PVT module is comprised of a copper absorber plate integrated with serpentine copper tubes soldered together and attached at the backside of the PV module using high thermal conductivity grease HP. High-performance insulation (type SLENTEX) was placed on the copper pipes, and an aluminium plate covered the PV module to minimize thermal losses. The PV modules have fixed with a tilt angle of 14.8° towards the south. Twenty-one thermocouples (T type) were used to measure the temperature on different points of the system; on each the surface and backside of the PV module and the PVT system, four thermocouples were distributed. Another thermocouple is placed at the inlet, outlet of the PVT system, the inside nanofluid tank, in the water tank and one for measuring the ambient temperature. The outlet of the PVT system is connected to a copper coil that was immersed inside the water tank, and the outlet of the coil is connected to the nanofluid tank. Figure 2 shows the experimental setup of the reference PV module and PVT system. Data logger of type National instrument model NI cDAQ-9178 consists of 24 channels and was used for measuring temperatures, voltages, currents of PV modules, solar radiation and flow rate. The data logger was connected with IN Signal Express 2015 software, recording and reading the data every 10 minutes. Table 3 shows the measurement devices and sensor specifications used.

Table 3. Specifications of measurement devices and sensors

Item	Model/Brand	Range	Accuracy
Thermocouples	T-type 0.2 mm	-250°C to 400°C	± 0.5 °C
Solar sensor	SS11.303	1-3999 W/m^2	± 0.1 W/m^2
Flow rate sensor	YF-S201	1-30 L/min	±10%
Electronic scale	BOECO BAS	3 kg	0.0001 g
Current sensor	ACS712	up to 30 A	0.04 A
Voltage sensor	Module 25V	up to 25 V	0.02445 V
Flow rate sensor	YF-S201	1-30 L/min	±10%
Pump	AD20P-1230C	240 L/H	---------
Ultrasonication	Bransonic	240V, Vf: 48 kHz	----------

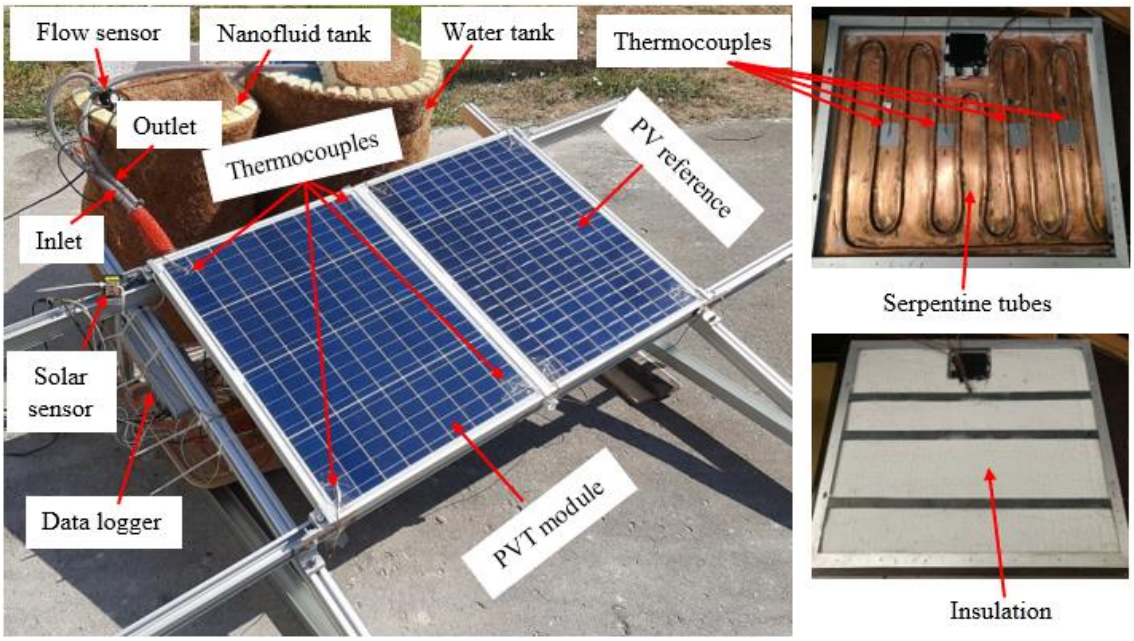

Figure 2. A sight of the experimental setup

3.2 Thermodynamic analysis

3.2.1 Energy evaluation

This section evaluates the PVT system's energy and exergy according to thermodynamics laws. The first law of thermodynamics is to evaluate the PVT system's performance by determining the energy quantity produced by the PVT system, including thermal and electrical efficiency. The electrical efficiency is affected by the voltage and current produced by PV cells due to the incident of solar radiation. Thereby the electrical power produced and solar radiation, in addition to the PVT system area, are the main parameters which affect the electrical efficiency; Eq (1) are applied to determine the electrical efficiency [9]. Thermal efficiency is the other efficiency produced by removing heat excess from the backside of the PV module, which is also affected by properties of fluid used, mass flow rate, and temperature difference with considering the solar radiation and system area.

$$\eta_{\mathrm{el}} = \frac{P_{out}\, FF}{\mathrm{AS}} \tag{1}$$

$$\mathrm{FF} = \frac{V_{\mathrm{mp}} I_{\mathrm{mp}}}{V_{\mathrm{oc}} I_{\mathrm{sc}}} \tag{2}$$

The average temperature T_{avg} is measured by Eq (12) which represents the average temperature of the surface and back side of the PVT system, which is measured by thermocouples.

$$T_{avg} = \frac{\mathrm{T_{surface} + T_{buck}}}{2} \tag{3}$$

where, P_{out} is the electrical power = ($V_{\mathrm{out}} \times I_{\mathrm{out}\,F}$), V_{out} output voltage, I_{out} output current and FF is the fill factor which represents the maximum electrical power conversion efficiency of the PV module [10], which is calculated from Eq. (2), (S) is the solar radiation and (A) PVT module area. The heat transfer from the backside of the PV module to the absorbing plate and then to the fluids circulating in tubes helps to remove the heat of the PV cells and then increase thermal efficiency; Eq. (4) is used to determine thermal efficiency [11].

$$\eta_{th} = \frac{\dot{m} C_p (T_{\mathrm{out}} - T_{\mathrm{in}})}{\mathrm{AS}} \tag{4}$$

where $\dot{m},\ C_p, T_{out}, T_{in}$ are the mass flow rate, specific heat of the fluid, inlet and outlet temperatures of the fluid, respectively. The overall efficiency is sum of thermal and electrical efficiencies, which can calculate from Eq. (5) [12].

$$\eta_{ov} = \eta_{el} + \eta_{th} \tag{5}$$

Thermophysical properties of the circulating fluid affect the heat transfer properties, which reflect the PVT performance. The flow pattern affects the heat removal rate during fluid circulation in tubes attached to the backside of the PV module. Reynolds number has been used to predict flow patterns depending on the mass flow rate $\dot{m}$, the viscosity of working fluid μ and hydraulic diameter D_h, which is calculated by Eq. (6) [13].

$$\mathrm{Re}_{nf} = \frac{4\dot{m}}{\pi \mu_{nf} D_h} \tag{6}$$

Nusselt number is the ratio of heat convection to heat conduction, which is determined with Eq (7) [14].

$$Nu_{nf} = \left(\frac{\mathrm{h} D_h}{K_{nf}}\right) = \frac{\dot{m} C_p (T_{h,i} - T_{h,\rho})}{\mathrm{A}(T_{avg} - T_{\mathrm{w}})} \times \frac{D_h}{K_{nf}} \tag{7}$$

where h, Tw are the heat transfer coefficient and the average wall tube temperature. The friction factor is a parameter that influences the pressure drop with a change in Reynold's number due to an increase in the viscosity and density because of the increase in the volume concentration in the base fluid. Equations (8) (9) are used to calculate both fraction factor and pressure drop [15][16].

$$f = [1.58 \ln\ Re - 3.82]^{-2} \tag{8}$$

$$\Delta P = \frac{f \rho_f L}{2 D_{\mathrm{tubes}}} \left(\frac{4 \frac{m_f}{n}}{\rho_f \pi D^2} \right)^2 \tag{9}$$

where n is the number of tubes and L is the riser length.

3.2.2 Exergy evaluation

The second law of thermodynamics evaluates the exergy quality of the PVT system [17], including the exergy efficiency, losses and entropy generation. Then determine the realistic performance of the PVT systems and evaluate the quality of their electrical and thermal exergy [18]. Evaluating the exergy of the PVT system requires knowing the control volume of the system as well as its input and output that affect the exergy of the PVT system, as shown in Figure 3. By supposing the PVT system is in semi-steady condition, the exergy balance of the system is expressed by Eq. (10) [19] below.

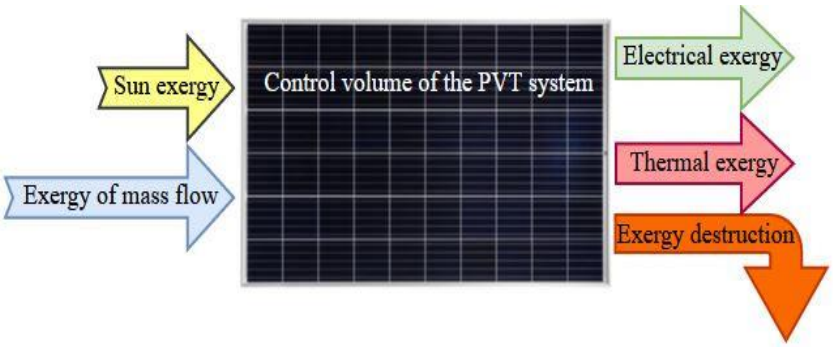

Figure 3. The exergy flow of a PVT system

$$\sum \dot{E}x_{\text{in}} = \sum \dot{E}x_{\text{out}} + \sum \dot{E}x_{\text{loss}} \tag{10}$$

The inlet exergy $\dot{E}x_{\text{in}}$ is the sum of solar exergy ($\dot{E}x_{\text{solar}}$) which represents the incident solar radiation absorbed by the PVT system, which calculates by Eq. (11) [20] and the cooling fluid inlet to the system.

$$\dot{E}x_{\text{in}} = \dot{E}x_{\text{sun}} = S\left(1 - \frac{T_{amb}}{T_{\text{sun}}}\right) \tag{11}$$

where T_{amb}, is the ambient temperature and $T_{sun}$is the sun temperature = (5800 K) [21]. The output exergy ($\dot{E}x_{\text{out}}$) is the sum thermal ($\dot{E}x_{\text{ther}}$) and electrical energy ($\dot{E}x_{\text{ele}}$), Thermal exergy is calculated by Eq. (12), [22]. The electrical exergy is equal to the electrical power energy produced [4], which can be calculated by Eq. (13).

$$\dot{E}x_{th} = \dot{m}\, C_{p,f}\left[\left(T_{f\ \text{out}} - T_{f\ \text{in}}\right) - T_{\text{amb}} \ln\left(\frac{T_{f\ \text{out}}}{T_{f\ \text{in}}}\right)\right] \tag{12}$$

$$\dot{E}x_{ele} = P_{pv}\ \text{FF} \tag{13}$$

Thereby, the PVT system's thermal and electrical exergy efficiencies can be calculated depending on Eqs. (14) and (15) [19].

$$\eta_{\dot{E}x_{ther}} = \frac{\dot{m}\, C_{p,nf}\left[\left(T_{f,\ \text{out}} - T_{f,\text{in}}\right) - T_{\text{amb}} \ln\left(\frac{T_{f\ out}}{T_{f\ \text{in}}}\right)\right]}{S\left(1 - \frac{T_{\text{amb}}}{T_{\text{sun}}}\right)} \times 100 \tag{14}$$

$$\eta_{\dot{E}x_{ele}} = \frac{P_{pv}\ \text{FF}}{S\left(1 - \frac{T_{\text{amb}}}{T_{\text{sun}}}\right)} \times 100 \tag{15}$$

The exergy efficiency is the sum of thermal and electrical efficiencies of the PVT system, which is calculated by Eq. (16).

$$\eta_{\dot{E}x} = \frac{\dot{E}x_{ther} + \dot{E}x_{ele}}{\dot{E}x_{\text{solar}}} \times 100 \tag{16}$$

The exergy destruction (exergy losses) is important the parameter occurs due to the frictional and heat transfer losses in the system. Entropy generation $\dot{S}_{\text{gen}}$ or irreversibility is a thermodynamic parameter that indicates the irreversibility occurs in the system [23]; both parameters can be calculated by Eqs. (17), (18) as follows:

$$\dot{E}x_{\text{losses}} = \dot{E}x_{\text{in}} - \dot{E}x_{\text{ele}} - \dot{E}x_{\text{ther}} \tag{17}$$

$$\dot{S}_{\text{gen}} = \frac{\dot{E}x_{\text{lost}}}{T_{\text{amb}}} \tag{18}$$

3.2.3 Thermophysical properties of nanofluids

Solid materials are characterized by higher thermal properties than liquids. Dispersion of a specific quantity of nanomaterials in the base fluid produces a new fluid with higher thermal

properties than base fluids. Thermal conductivity, specific heat, density, and viscosity are the most effective properties that significantly affect the nanofluid performance. The density of the nanofluid is an essential property which affects nanofluid stability and the thermal system's sustainability; Eq. (19) is used to calculate the density of nanofluid [24]. The thermal conductivity of nanofluid has a significant effect on the heat transfer field and increasing this property help enhance the thermal performance of nanofluid, which can calculate from Eq. (20) [25]. The specific heat has a vital role in providing the energy that transmits from one body to another. The specific heat of nanofluid depends on the type of nanomaterials used, the type of base fluids, and their concentration in the base fluid. Equation (21) is used to calculate the specific heat of the nanofluid [26]. Viscosity is not less important than density, which has essential effects on the nanofluids' behaviour and pumping power of the thermal system; Eq. (22) is used to calculate the viscosity of nanofluids [27]. Table 4 shows the thermophysical properties of mono and hybrid nanocomposites.

Table 4. The properties of the nanomaterials and DI water

Properties	Fe_2O_3 [28]	WO_3 [29]	TiO_2 [28]	CuO [30]	ZrO_2 [31]	TiO_2-Fe_2O_3	TiO_2-CuO
Density (kg/m^3)	5240	7160	3900	6310	5890	3473	2791
Thermal conductivity (W/m·K)	20	1.63	8.9	32.9	2.7	75.32	79.9
Heat capacity (J/kg·K)	650	335	686	551	0.455	1321	1121

$$\rho_{nf} = \phi \cdot \rho_{np} + (1-\phi) \cdot \rho_{bf} \tag{19}$$

$$\frac{k_{nf}}{k_{bf}} = \frac{k_{np}+2k_{bf}+2\emptyset(k_{np}-k_{bf})}{k_{np}+2k_{bf}-\emptyset(k_{np}-k_{bf})} \tag{20}$$

$$C_{p,nf} = \frac{\phi\cdot(\rho_{np}\cdot C_{p,n})+(1-\phi)\cdot(\rho_{bf}C_{p,bf})}{\rho_{nf}} \tag{21}$$

$$\mu_{nf} = \frac{\mu_{bf}}{(1-\phi)^{2.5}} \tag{22}$$

$$\phi = \left[\frac{\frac{m_{\mathrm{ap}}}{\rho_{np}}}{\frac{m_{\mathrm{np}}}{\rho_{\mathrm{np}}}+\frac{m_{\mathrm{bf}}}{\rho_{bf}}}\right] \times 100 \tag{23}$$

where k_{np}, k_{nf}, k_{bf}, are the thermal conductivity of nanomaterials, nanofluid and base fluid respectivly. ϕ is the volume concentration of nanomaterials dispersion in the base fluid, m_{bf} m_{np} are the mass of the base fluid and nanomaterials. $C_{p,nf}$, $C_{p,np}$, $C_{p,bf}$ are the specific heat of the nanofluid, nanomaterials and base fluid and respectively. while ρ_{np} ρ_{nf}, ρ_{bf}, are the density of nanomaterials, nanofluid, and base fluid.

3.2.4 Preparation of nanofluids

In this dissertation, various types of nanofluids have been prepared, such as WO_3/DI water, ZrO_2/DI water, TiO_2/DI water, Fe_2O_3/DI water, CuO/DI water nanofluids, and two types of hybrids nanofluids such as TiO_2-CuO/DI water, TiO_2-Fe_2O_3/DI water. The two-type method is employed to prepare nanofluids at different volume concentrations dispersed in DI water were calculated from Eq. (23). The quantity of nanomaterials was scaled by an electronic scale (type: BOECO BAS of 0.0001g), then dispersed into DI water and mixed with a magnetic stirrer for a different period among 25-30 min depending on the type of nanomaterial employed. Ultra-sonication probe (Bransonic type 220, Voltage: 240V, Vf: 48kHz) was used from 35-40min depending on the type of nanomaterial employed to avoid the agglomeration of nanoparticles

in the nanofluid and to obtain a stable suspension for a long period, as shown in Figure 4. The time sediment and visualization methods were used to examine the nanofluid's stability for different periods from 3-5 h after sonication and from 2 to 4 days after sonication. Thus, it was prepared in suitable quantities later and directly used in the experiment after the sonication.

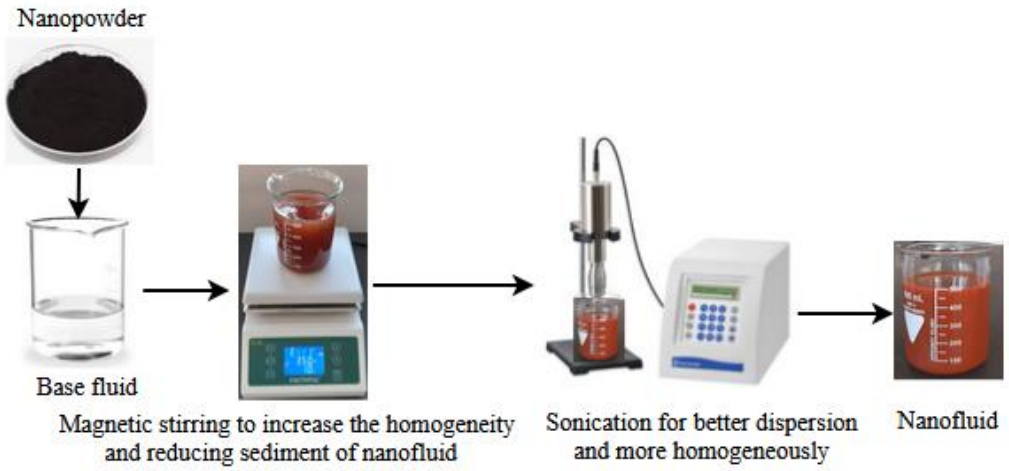

Figure 4. Preparation of nanofluid by using two steps method

4. New scientific results

4.1 A numerical simulation to predict the thermal and electrical behaviour of the PV module at different operation conditions.

Contribution 1

(a) The first case study is characterized by using predicted equations that can be adopted to test the PV module's thermal behaviour under different conditions and give a general impression of temperature distribution on the PV module. Also, simulation was conducted according to the material properties of the PV module layers, such as thermal conductivity, densities, and specific heat for each layer, which give more precise heat transfer depending on the characteristics of each layer. The solar radiation values have been calculated depending on the mathematical equations for January and July of Miskolc city. It was found that the thermal behaviour of the PV module is a variable with solar radiation change during the day, which was clear by temperature distribution on the PV module surface. The low the solar radiation value and temperature (176 W/m^2, 4 °C), the lower the intensity of solar radiation affects the PV module's short circuit current by the number of photons absorbed by the semiconductor material that PV cells are made from then, influenced by the PV module performance. The average temperature at the solar radiation and temperature mentioned above was 15.2 °C, and this temperature level is not causing damage to the PV module but reducing their electrical power and efficiency. Increasing solar radiation and temperature to (734 W/m^2, 35 °C) causes an increase in the PV module temperature that causes reduce in power output with damage to PV cells at continuously increased temperatures. An increase in the ambient temperature causes an increase of PV cells, which leads to a significant decrease in open-circuit voltage when the PV module temperature is above 25 °C with a slight drop by short circuits current, then a reduction in power output. Rising temperature to 82 °C causes degradation of the PV module performance and causes appearing of local hotspots when the temperature reaches the extreme range, which requires cooling of PV cells to remove the excessive heat and sustain its work. This case study help

identify the problems faced by PV cells work and then determine the effective technique that improves PV performance.

(b) In the second case, we have modelled the PV module through equations that can control as one system undergoes controllable inputs and outputs that depend on the parameters we are setting. This investigation helps to predict the electrical behaviour of the PV module depending on input parameters and then identify the appropriate parameters that could achieve better electrical performance. The simulation considers variable and constant values of solar radiation and temperature as input to observe output voltage and current and power of the PV module as outputs. It found that reducing the solar radiation less than STC, even with 35 °C, reduces the current and voltage of the PV module to 21.52% and 13.63 %, respectively. Constant temperature with a gradual lowering of solar radiation is a significant effect by reducing the current and voltage of the PV module, which confirms the importance of the intensity of solar radiation on power produced. Constant solar radiation values and gradually lowering temperature has a slight effect on the current of the PV module and a higher effect by reducing the voltage compared with constant temperature and variable solar radiation. It was found that decreased temperature of the PV cells with constant solar radiation has a slight effect on the PV module performance. The second case has confirmed the effect of the intensity of solar radiation and temperature on the open-circuit voltage and short-circuit current that affects the PV module performance.

4.2 The effect of evaporating cooling on thermal and electrical behaviour under a hot climate

Contribution 2

The passive cooling applied showed sustained performance of the PV modules in hot conditions. The CWIWs technique has good potential cooling to control the heat of the PV module, lower cost, and has an easy configuration with less water consumption. The CWIWs attached to the backside of the PV module are effective passive cooling techniques that contributed to reducing the PV module temperature by 22% compared with the PV module without cooling. The moist condition resulting from the cotton bristles immersed in water and exposure to the wind has provided appropriate cooling that enhances efficiency to 7.25 % and the power yield increment of about 16.3 W, as shown in figure 5 a. Using CWIWs decreases the entropy generation of the PV module by 14.32% due to reducing the losses exergy by 14% of the PV module compared to the PV module without cooling. The electrical energy (output power) was the same as the electrical exergy, and the exergy efficiency of the PV module with evaporating cooling was higher than the PV module without cooling, as shown in figure 5 b. The passive cooling applied enhanced the performance of the PV module higher than in another similar study, making it more reliable for application. Significant power yield deterioration and the PV modules' efficiency were observed due to the PV cell's temperature increase to 56.4 °C.

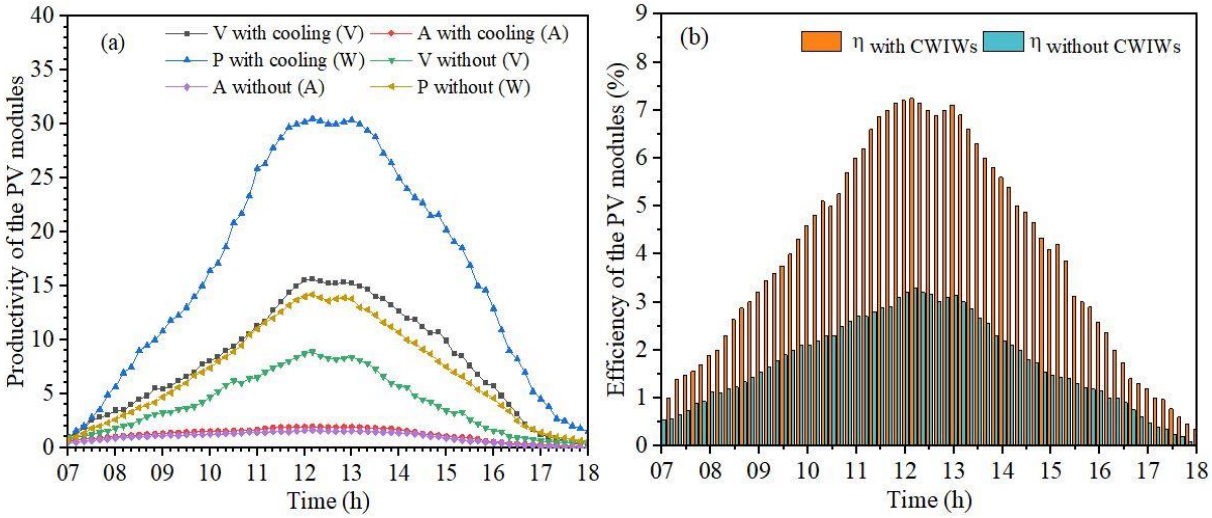

Figure 5. The variation value of (a) productivity of PV modules and (b) Efficiencies of the PV modules with and without CWIWs

4.3 Experimental comparative study on using different cooling techniques with PV module

Contribution 3

The study compared passive (CWIRAF) and active cooling (circulated water) techniques to enhance the PV module's performance. Increasing the heat dissipation area of the back surface of the PV module by aluminium fins integrated with wet cotton bristles and exposed to the air created a cooling environment during the experiment period. The cooling techniques applied showed sustained performance of the PV modules under hot conditions. The CWIRAFs passive cooling technique shows improved behaviour and significantly enhances the PV module performance by lowering its temperature under hot conditions using minimal equipment. Increasing the heat dissipation area of the back surface of the PV module by aluminium fins integrated with wet cotton bristles and exposed to the air created a cooling environment during the experiment period. Thereby contributing to lowering the PV module's average temperature by 137.7% than the active cooling technique. The passive cooling applied in this work effectively reduces the PV module temperature and improves its performance better than in other studies, which makes it more reliable. A reduction in PV module temperature using the CWIRAF technique increased the power yield and efficiency by 13.78% and 8.86%, respectively, compared with the PVT collector. The active cooling technique showed lower performance than passive cooling under similar conditions. This result is attributed to heat transfer across different PVT collector layers, not directly, such as CWIRAFs cooling. The PVT collector enhances thermal energy by removing excess heat from the PV module's backside by circulating water inside pipes, improving the overall efficiency of the PVT collector. The PV modules used without cooling in hot climate conditions significantly deteriorated their performance. Figure 6 shows the performance of the PV module under different cooling techniques. The economic analysis of the PVT system has achieved a good payback period within a short period compared with the conventional reference PV module, which confirms the feasibility of the cooling approach used. The cooling technique applied may be feasible for small installations of PV modules, such as a family house system. In future work, the research domain will consider more extended experimental periods with the help of numerical tools and suggest improvements for reducing water consumption.

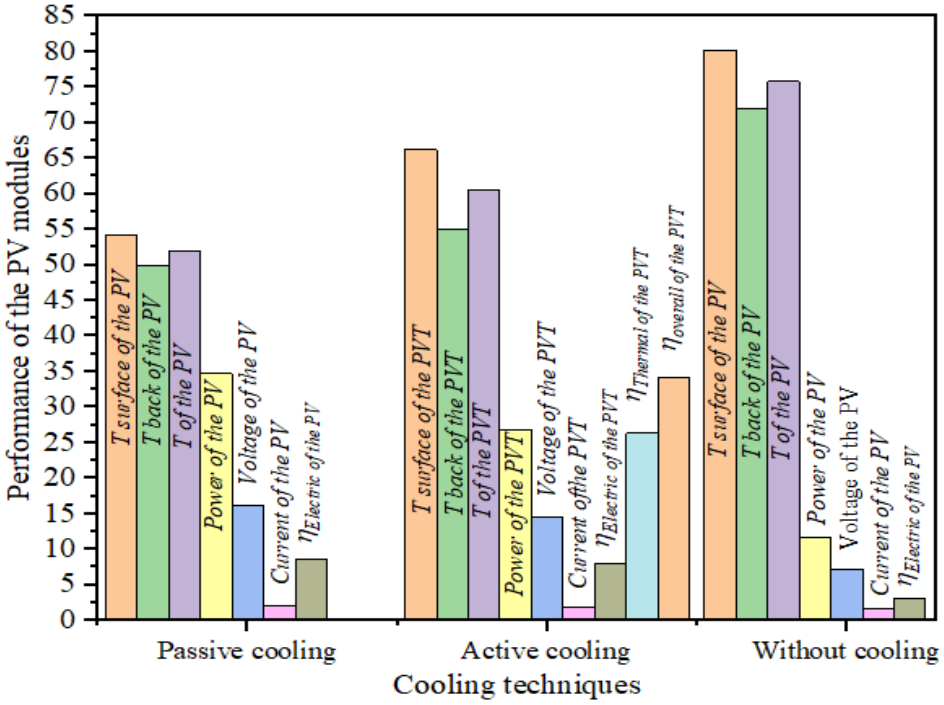

Figure 6. Comparison of PV modules performance under different cooling techniques

4.4 Effect of active cooling on energy and exergy of PVT system using WO_3 and ZrO_2 nanofluids: An experimental study

Contribution 4

The increased volume concentration of WO_3 nanoparticles in the base fluid reduced the PV module temperature due to enhanced WO_3 nanofluid thermal conductivity compared to DI water. Thus, the reduced PV module temperature has positively improved electrical power generation. The increased volume concentration of WO_3 nanoparticles in DI water reduced the temperature of the PV cells by 21% has enhanced the electrical power by 62% due to improved heat transfer coefficient compared with DI water, which increased the electrical efficiency of the PVT system by 52%. The increase in volume concentration gradually increased the thermal efficiency of the PVT system by 30.1%, as shown in figure 7. Nusselt number and the heat transfer coefficient of the WO_3 nanofluid were improved by 51.2% and 5.3% with the increase of the volume concentration and Reynolds number due to the increased nanofluid density and viscosity. Increasing volume concentration and Reynolds number has increased the pressure drop by 49.2% compared to DI water.

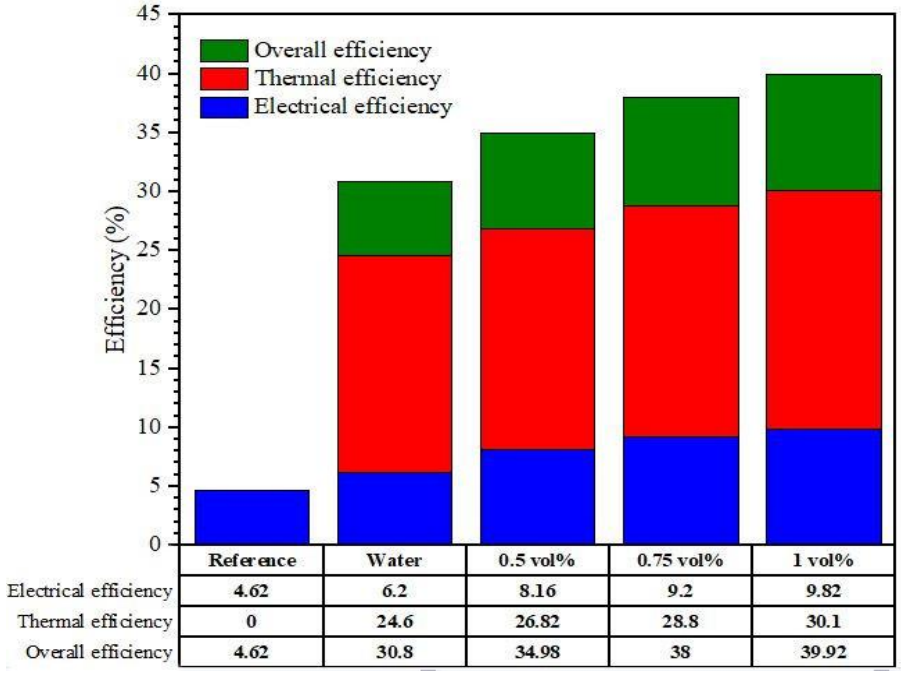

	Reference	Water	0.5 vol%	0.75 vol%	1 vol%
Electrical efficiency	4.62	6.2	8.16	9.2	9.82
Thermal efficiency	0	24.6	26.82	28.8	30.1
Overall efficiency	4.62	30.8	34.98	38	39.92

Figure 7. The overall efficiency of the PVT systems against the reference PV module

The thermal exergy of the PVT system was lower than the electrical exergy due to the convergence of the fluid outlet temperature of the PVT system to the ambient temperature. Increasing the volume concentrations of WO_3 nanofluid achieved a relative increment of the thermal exergy compared to the cooling by DI water. The thermal exergy efficiency of the PVT system was low due to the drop in the quality of the thermal exergy. Thus, an increased volume concentration has positively influenced the thermal and electrical exergy efficiencies due to the enhanced nanofluid heat transfer coefficient. Figure 8 shows the effect of using WO_3 nanofluids reduced the exergy loss and entropy generation by 15.32% and 53.5% because of their heat transfer enhancement and reduced fluid friction in PVT systems.

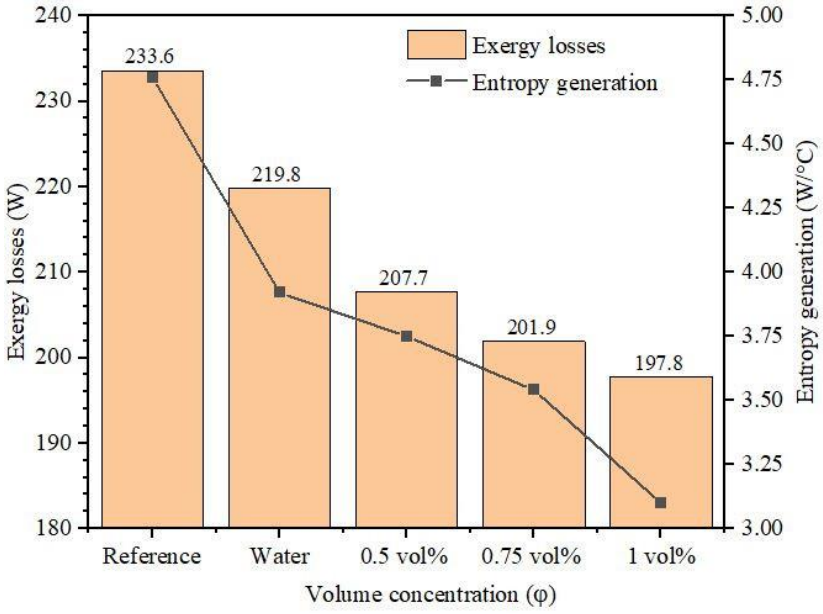

Figure 8. Exergy losses and entropy generation of the PVT system at different concentrations against the PV module

Contribution 5

Different volume concentrations of ZrO_2 nanoparticles have been applied in water to investigate their effect on heat transfer coefficient, Nusselt number fraction factor and pressure drop compared with water as a coolant. Improving the thermal conductivity of ZrO_2 nanofluid leads to increasing the heat absorption at the backside of the PV module, then reduces the PV module temperature to 21.2% compared to water. Reduced the PV module temperature effectively increased the electrical power to 33.72 W. The electrical and thermal efficiency was enhanced by using nanofluids, which positively reflected the overall efficiency of the PVT system increased to 60% compared with water at 0.0275 vol%. Increased nanoparticle concentration increased the thermal conductivity of nanofluids, and then more heat was absorbed from the PV module. Increasing the volume concentration of ZrO_2 nanoparticles in base fluid and Reynolds number has enhanced the heat transfer coefficient and Nusselt number due to the increase in the thermal conductivity of the nanofluid. On another side, the density and viscosity have increased, which causes reduced friction factors and increased pressure loss. Exergy analysis indicates lower thermal exergy of the PVT system than electrical exergy, which is attributable to the closing of the fluid outlet temperature of the PVT system to the ambient temperatures. Despite that, a remarkable relative increment of the thermal exergy has been found with increases in the volume concentrations of ZrO_2 nanofluid compared with water. The overall exergy efficiency is affected by the thermal and the electrical exergy efficiencies, which incremented with using nanofluid by 11.86 at 0.0275 vol% compared with water due to the high thermal conductivity enhancing of the convective heat transfer. Exergy losses and energy generation has reduced by 7 % and 26% at 0.0275 vol% compared to water because of their effects on convective heat transfer. The PV module, without cooling, is exposed to significant degradation in its performance.

4.5 Effect of mono nanofluids TiO_2, CuO, and Fe_2O_3 nanofluids on the PVT system performance: An experimental study

Contribution 6

Dispersion of CuO nanofluid at different volume concentrations for cooling the PVT system gives good results, which improves the PVT system performance. Copper oxide nanoparticles are characterized by higher thermal conductivity, which is positively reflected by a reduced PVT system temperature of 23.44%. Reduced PVT system temperature helped increment the electrical power from 20.78 W to 35.47 W at 0.3 vol%, thus enhancing the electrical efficiency from 5.43% to 10.3%, which confirms the effectiveness of the nanofluid used. The CuO nanofluid thermal properties helped to improve the heat transfer coefficient, which led to more absorption of excess heat from the backside of the PVT system, then increased the thermal efficiency to 38.9%. Most studies use TiO_2 nanoparticles to prepare nanofluids as a cooling fluid for different PVT system configurations; in the current case, TiO_2 nanowires have been adopted, which are characterized by having a surface area to help increase heat absorption. Compared with the reference PV module, using TiO_2 nanofluid decreased the PVT system temperature to 14% at 0.3 vol% and increased the electrical power to 49.7%. Reduced temperature and increment of electrical power improve the electrical PVT system efficiency by 27.5%, while increased thermal conductivity of nanofluid increases heat absorbing from PV cells and then increases thermal efficiency to 34.6%.

Suspension of 0.3 vol% of Fe_2O_3 nanoparticles in DI water improved the convection heat transfer, which helped to reduce the PVT system temperature by 29.64%. Compared with DI water, the electrical power increased from 21.37 W to 37.76 W, that is, by 76.68%, enhanced the electrical power positive reflected to increase the electrical efficiency to 12.1% at increased the volume concentration to 0.3 vol%. Thermophysical properties of Fe_2O_3 nanoparticles

significantly help to improve the heat transfer convection between the backside of the PV module and the heat exchanger, then increase heat removal from the PV cells, thus increasing the thermal efficiency to 43.3%. Table 5 shows the effect of different cooling fluids on the PVT system, which contributes to reducing the PV cell temperature and increasing the efficiency of the PVT system higher than DI water. At 0.3 vol%, the Fe_2O_3 nanofluids achieved better performance by reducing the temperature, incrementing electrical power, and increasing electrical and thermal efficiency more than other nanofluids. This is attributed to the high thermal conductivity of Fe_2O_3 nanofluids compared to CuO and TiO_2 nanofluids, which help increase the heat transfer convection between nanofluids and tubes, which is reflected by reducing the PVT system temperature. CuO nanofluid achieved higher performance than TiO_2 nanofluid because of their high thermal properties, which positively reflected the PVT system performance.

Table 5. Effect of different nanofluids on the PVT system performance

Cooling applied	PV_{ref}	Cooling by DI water	PV_{ref}	Cooling by CuO nanofluid	PV_{ref}	Cooling by TiO_2 nanofluid	PV_{ref}	Cooling by Fe_2O_3 nanofluid
T_{PV} °C	55.6	-	52.86	-	52.57	-	50.9	-
T_{PVT} °C	-	55.6	-	42.82	-	46.11	-	39.26
P_{PV} W	19.3	-	20.78	-	21.15	-	21.37	-
P_{PVT} W		22.19		35.47	-	31.66	-	37.76
η_{ele-PV} %	5.11	-	5.42	-	4.89	-	5.75	-
$\eta_{ele-PVT}$ %	-	6.32	-	10.3	-	8.44	-	12.1
$\eta_{ther-PVT}$ %	-	30.25	-	49.2	-	43	-	55.4

4.6 The effects of new hybrid nanofluids TiO_2-CuO and TiO_2-Fe_2O_3 on the energy, exergy efficiency of the PVT system

Contribution 7

The hybrid TiO_2-Fe_2O_3 nanofluid consisting of 50% nanowires and 50% nanoparticles has created a new hybrid nanofluid having new thermophysical properties that help improve the hybrid nanofluid performance used with PVT system more than mono nanofluid. Loading TiO_2 NWs over Fe_2O_3 NPs has increased the surface area of the nanocomposite, which positively reflected heat absorbing and then enhanced the PVT system performance. Compared to the reference PV module, circulation of DI water decreased the PV module temperature by 9.67%, using hybrid nanofluid at 0.2 vol%, 0.3 vol% reduced the PV module temperature by 25% and 33.63%. Due to decreased PV cell temperature, the PVT system's electrical power has increased by 17.63%, 68.32% and 71.6% at DI water and hybrid nanofluids, respectively. Increment in the electrical power has enhanced the electrical efficiency of the PVT systems to 7.1%, 12.44%, and 12.62% at cooling by DI water and hybrid nanofluid at different volume concentrations compared with the reference PV module, as shown in figure 9 a. Increasing the volume concentrations by 0.2 vol% and 0.3 vol% in the base fluid has increased the nanofluid heat transfer coefficient and heat removal from the PV cells, then enhanced the thermal efficiency of the PVT system by 39.26% and 47.85% compared to used DI water, as shown in figure b. Compared with DI water, using a hybrid nanofluid enhanced the Nusselt number by 25 % at 0.3 %vol. An increase in Nusselt numbers has positively increased the heat transfer coefficient by 43.33% at 0.3 vol%, which helped lower PV temperature and increased thermal efficiency. Increased volume concentration causes increased nanofluid density and effect by the pressure drop of about 36.12%; increased Reynolds number and volume concentrations lead to dropping the fraction factor to 10.52%.

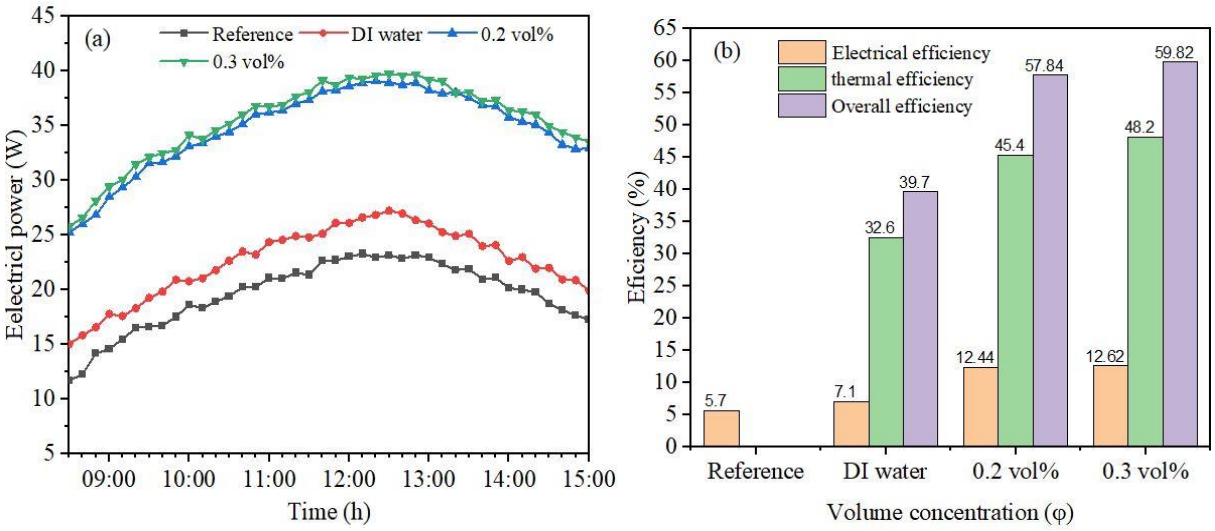

Figure 9. Performance of the PV and PVT system (a) electrical power, (b) overall efficiency

The thermal exergy is affected by the specific heat of the cooling fluid, flow rate and temperature. An increase in the TiO_2-Fe_2O_3 nanocomposite in base fluid increments the thermal exergy by 17.29% and 13.87% compared to DI water. The relative increase of the volume concentrations increments the thermal exergy efficiency to 2.43%, 2.28% compared with DI water, which was lower than electrical exergy efficiency due to the low quality of the thermal exergy. Increment of electrical exergy has a positive reflection to enhance the electrical exergy efficiency of the PVT system by 69.4% and 82.3% compared to cooling by DI water, which significantly increments the overall exergy of the PVT system by 79.1% and 66.67%, even with a relative increment in thermal exergy efficiency. The exergy losses increase with the rising PV module temperature. Compared to cooling by DI water, employing hybrid nanofluid help in reducing the exergy losses by 13.57% and 42.33%. Thereby reducing entropy generation by 60.9% and 70.47%, which contributes to reducing the work lost in the PVT system. Compared with previous studies, which adopted different sizes of the PVT system, the nanofluids and volume concentrations of the nanocomposite. The employed hybrid TiO_2-Fe_2O_3 nanofluid enhanced the energy and exergy of the PVT system better than previous studies, confirming the effectiveness of the hybrid nanofluid employed. The economic analysis of cooling by hybrid nanofluid achieved a satisfying payback period for the PVT system, which produces electrical and thermal energy compared to the reference PV module with a difference of more than 3 months.

Contribution 8

Energy and exergy of the PVT system have been conducted to evaluate the quantity and quality of the PVT system's productivity. The effectiveness of the hybrid nanofluid at different volume concentrations helps to extract the excessive heat and reduces PV module temperature by 36.1% and 39%, while DI water by 5.6 % compared with the reference PV module. The electrical power improved of the PVT system by 73.95% and 77.5% at increased volume concentrations due to improving the hybrid nanofluid's thermal properties, while using DI water improved it by 10.4%. Thus, the electrical efficiency of the PVT system increased by 12.28% and 12.4%. The high thermal characteristics of hybrid nanofluids increment heat transfer convection and then improve the thermal efficiency of the PVT system to 56.48% and 58.2%, then increment the overall efficiency of the PV module, reaching 36.25% and 56.48%. Convergence of the outlet fluids temperature with ambient temperature causes decreased thermal exergy and thus reduced thermal exergy efficiency. Cooling by hybrid nanofluid has improved the electrical exergy efficiency by 11.33 % and 12.18%, while a slight improvement was recorded using DI

water. The overall exergy efficiency has increased to 13.44 %, 14.97 % and 6.28 % at different nanocomposite volume concentrations and DI water. The exergy losses were reduced by 32.3% and 37.9% due to enhancing the thermal characteristics of hybrid nanofluids, while used DI water was reduced by 4.5% compared to the reference module. The effective cooling by hybrid nanofluid causes reduced entropy generation by 62.2 % and 69.6%, compared with DI water. Improving the performance of nanofluids positively reflected in their performance the TiO_2 nanofluid was less effective than CuO and Fe_2O_3 nanofluids. Thus, loading Fe_2O_3 nanorods over TiO_2 nanowires and loading CuO nanoparticles over TiO_2 nanowires produced new hybrid nanocomposites with high thermal properties than mono nanomaterials. Dispersion of the hybrid nanocomposites in DI water achieved high performance than the mono nanofluids; Table 6 shows the improvement of the PVT system at 0.3 vol% of TiO_2-Fe_2O_3 and TiO_2-CuO nanofluids compared with mono nanofluid used, as mentioned in Table 15. Using TiO_2-Fe_2O_3 nanofluid achieved higher performance than TiO_2-CuO due to the high specific heat and low density of Fe_2O_3 nanorods that help to enhance the thermal properties of the TiO_2 nanowire, and the results in Table 6 confirm the effectiveness of hybrid nanofluid as a cooling fluid.

Table 6. Effect of hybrid nanofluid on the PVT system performance

Cooling applied	PV_{ref}	Cooling by TiO_2-Fe_2O_3 nanofluid	PV_{ref}	Cooling by TiO_2-CuO nanofluid
T_{PV} °C	49.85	-	51.63	-
T_{PVT} °C	-	36.37	-	37.1
P_{PV} W	23.14	-	21.9	-
P_{PVT} W		39.71		38.88
η_{ele-PV} %	5.7	-	5.8	-
$\eta_{ele-PVT}$ %	-	12.62	-	12.4
$\eta_{ther-PVT}$ %	-	59.82	-	58.2

4.7 A numerical simulation of effect mono and hybrid nanofluids as cooling fluids on performance system PVT system

Contribution 9

Dispersion of nanomaterials in base fluid improves the thermophysical properties of cooling fluid higher than ID water, then accelerates heat exchange between circulated nanofluids in tubes and absorbs plate, which positively reflects on decreasing the PV cells temperature. The PVT system temperature decreased by 14.75% at cooling with ZrO_2 nanofluid at 0.0275 vol% and by 20.7% by cooling with hybrid nanofluid at 0.3 vol%. Improving the thermal properties of nanofluid help increase heat absorption and reduces the PV cell's temperature, which affects by increased energy and exergy efficiency. Reduction of the PV cell's temperature increased their electrical and thermal efficiency, as shown in figure 10 a and b attributed to the improvement of the heat transfer coefficient between the absorbing plate, which has a low temperature, and the backside of the PV module, which has a high temperature. The heat exchange helped decrease the temperature and increased the electrical efficiency to 55.6% and 76.8% using ZrO_2 and TiO_2-Fe_2O_3 nanofluid. The heat absorption by absorb plate has maximized the thermal efficiency of the PVT system by 15% of ZrO_2 nanofluid and 28.29% of TiO_2-Fe_2O_3 hybrid compared to DI water. Because the solid material has higher thermal properties than fluids, the dispersion of nanomaterials in DI water improves the thermal properties of the nanofluid. The thermal parameters have improved with an increased volume concentration of nanofluid; increasing of Nusselt number led to an increase of heat transfer coefficient by 12.34 % at used ZrO_2 nanofluid and 43.33% with hybrid nanofluid. An increase in volumetric concentration affects the pressure drop due to an increase in the nanofluid density,

then increased the pressure drop by 18.7% using ZrO_2 nanofluid, while using TiO_2-Fe_2O_3 nanofluid increased the pressure drop to 35.12%. The exergy efficiency of the PVT system improved with the dispersion of nanomaterial in the DI water, which caused of increase in the exergy efficiency of the PVT system due to improving heat exchange between the heating body of the PV module backside and absorber plate, which has low temperature. Thus, improving the thermal conductivity of nanofluid helped to increase the electrical exergy by 10.324% with ZrO_2 nanofluid, while using hybrid nanofluid enhanced electrical exergy to 12.62%, as shown in figure 10. The low quality of the thermal exergy due to the closer of the outlet temperature to the ambient temperature, which affected the thermal energy of the PVT system. For validating the simulation result work, a comparison study has been implemented between the simulation results and the experimental results, as shown in Table 7 below, and it was observed reasonable conformity between the numerical results and the experimental results.

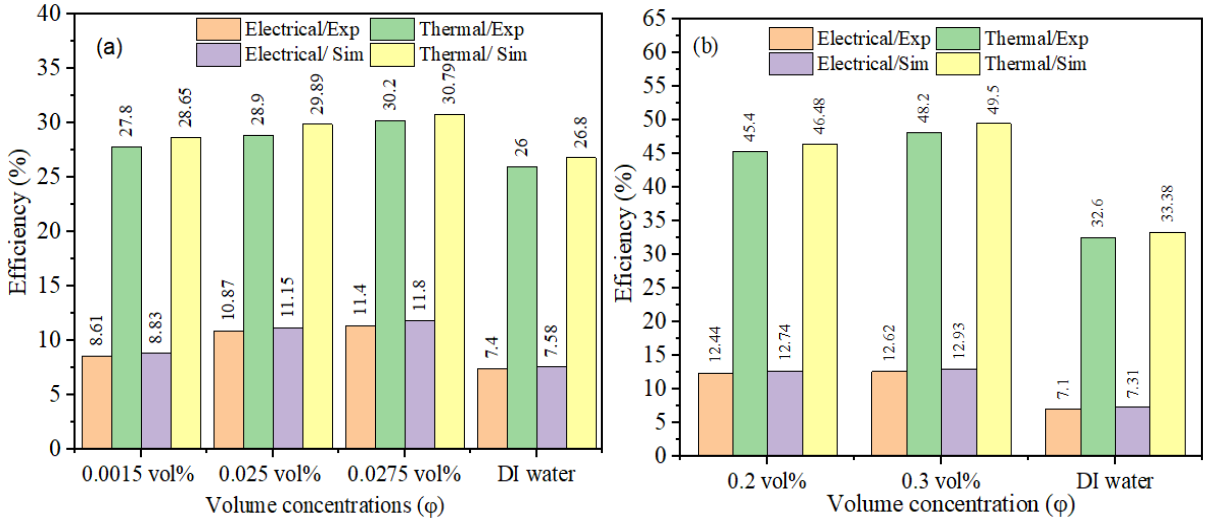

Figure 10. The electrical and thermal efficiencies of the PVT system cooled by (a) ZrO_2 nanofluid and (b) hybrid TiO_2-Fe_2O_3 nanofluid

Table 7. The variation between simulation and experiments results

Nanofluid	Temperature	Electrical efficiency	Thermal efficiency	Heat Transfer coefficient	Nusselt number	Pressure drops	Electrical exergy efficiency	Thermal exergy efficiency
ZrO_2	2.86%	3.61%	2.95	2.46	2.56	3.1	2.61	2.87
TiO_2-Fe_2O_3	2.73%	2.98%	3.1	2.3	2.96	2.6	3.12	3.3

Publications related to the dissertation

Articles Journals

[J1] Alktranee, M. & Péter, B. Energy and exergy analysis for photovoltaic modules cooled by evaporative cooling techniques. Energy Reports 9, 122–132 (2023).
[J2] Alktranee, M. et al. Energy and Exergy Assessment of Photovoltaic-Thermal System Using Tungsten Trioxide Nanofluid: An Experimental Study. Int. J. Thermofluids 100228 (2022).
[J3] Alktranee, M. et al. Effect of Zirconium Oxide Nanofluid on the Behaviour of Photovoltaic-Thermal System: An Experimental Study. Energy Reports 9, 122–132 (2023).
[J4] Alktranee, M. & Bencs, P. Experimental comparative study using different cooling techniques with photovoltaic modules. Journal of Thermal Analysis and Calorimetry. 2023.
[J5] Alktranee, M. & Bencs, P. Effect of Evaporative Cooling on Photovoltaic Module Performance. Process Integr. Optim. Sustain. 1–10 (2022)
[J6] Alktranee, M. & Bencs, P. Applications of nanotechnology with hybrid photovoltaic/thermal systems: A review. J. Appl. Eng. Sci. 19, 292–306 (2021).
[J7] Alktranee, M. & Bencs, P. Test the mathematical of the photovoltaic model under different conditions by using Matlab–Simulink. J. Mech. Eng. Res. Dev. 43, 514–521 (2020).
[J8] Bencs, P. & Alktranee, M. The potential of vehicle cooling systems. Journal of physics: Conference series vol. 1935 12012 (IOP Publishing, 2021).

Articles in Hungarian journals

[J1] Alktranee, M. & Bencs, P. Simulation study of the photovoltaic panel under different operation conditions. ACTA IMEKO 10, 62–66 (2021).
[J2] Alktranee, M. & Bencs, P. Overview of the hybrid solar system. Analecta Tech. Szeged. 14, 100–108 (2020).
[J3] Bencs, P., Al-Ktranee, M. & Mészáros, K. M. Effects of solar panels on electrical networks. Analecta Tech. Szeged. 14, 50–60 (2020).
[J4] Péter, B., Dávid, F. & Alktranee, M. Áramlás-és Hőtechnikai fejlesztések az EFOP-361 projekt keretében. Multidiszcip. Tudományok 11, 107–115 (2021).

Conferences participation

[C1] Spring wind conference, Hungary, 28 of May 2021.
[C2] International conference on vehicle and automotive engineering (VAE 2022) 8-9 September 2022, Miskolc, Hungary.
[C3] 17th Miklós Iványi International PhD and DLA Symposium 25-26 Oct, Pécs, Hungary 2021
[C4] 5th Agria Conference on Innovative Vehicle Technologies and Automation Solutions InnoVeTAS 2021 Digitization is the new normal, Hungary, 13th May 2021.
[C5] International Conference on Vehicle and Automotive Engineering (VAE2022) 8-9 September 2022, Miskolc, Hungary

References

[1] A. S. Abdelrazik, F. A. Al-Sulaiman, R. Saidur, and R. Ben-Mansour, "A review on recent development for the design and packaging of hybrid photovoltaic/thermal (PV/T) solar systems," *Renew. Sustain. Energy Rev.*, vol. 95, pp. 110–129, 2018.

[2] P. A. Østergaard, N. Duic, Y. Noorollahi, H. Mikulcic, and S. Kalogirou, "Sustainable development using renewable energy technology," *Renewable Energy*, vol. 146. Elsevier, pp. 2430–2437, 2020.

[3] A. Dawar, A. Wakif, T. Thumma, and N. A. Shah, "Towards a new MHD non-homogeneous convective nanofluid flow model for simulating a rotating inclined thin layer of sodium alginate-based Iron oxide exposed to incident solar energy," *Int. Commun. Heat Mass Transf.*, vol. 130, p. 105800, 2022.

[4] T. T. Chow, G. Pei, K. F. Fong, Z. Lin, A. L. S. Chan, and J. Ji, "Energy and exergy analysis of photovoltaic-thermal collector with and without glass cover," *Appl. Energy*, vol. 86, no. 3, pp. 310–316, 2009, doi: 10.1016/j.apenergy.2008.04.016.

[5] A. Ndiaye, C. M. F. Kébé, A. Charki, P. A. Ndiaye, V. Sambou, and A. Kobi, "Degradation evaluation of crystalline-silicon photovoltaic modules after a few operation years in a tropical environment," *Sol. energy*, vol. 103, pp. 70–77, 2014.

[6] N. Kahoul, H. Cheghib, M. Sidrach-de-Cardona, B. C. Affari, M. Younes, and Z. Kherici, "Performance degradation analysis of crystalline silicon solar cells in desert climates," *Energy Sustain. Dev.*, vol. 65, pp. 189–193, 2021.

[7] S. Lasfar *et al.*, "Study of the influence of dust deposits on photovoltaic solar panels: Case of Nouakchott," *Energy Sustain. Dev.*, vol. 63, pp. 7–15, 2021.

[8] J. C. Mojumder, W. T. Chong, H. C. Ong, and K. Y. Leong, "An experimental investigation on performance analysis of air type photovoltaic thermal collector system integrated with cooling fins design," *Energy Build.*, vol. 130, pp. 272–285, 2016.

[9] M. Hosseinzadeh, M. Sardarabadi, and M. Passandideh-Fard, "Energy and exergy analysis of nanofluid based photovoltaic thermal system integrated with phase change material," *Energy*, vol. 147, pp. 636–647, Mar. 2018, doi: 10.1016/j.energy.2018.01.073.

[10] M. Chandrasekar and T. Senthilkumar, "Passive thermal regulation of flat PV modules by coupling the mechanisms of evaporative and fin cooling," *Heat Mass Transf. und Stoffuebertragung*, vol. 52, no. 7, pp. 1381–1391, 2016, doi: 10.1007/s00231-015-1661-9.

[11] Y. Yu, E. Long, X. Chen, and H "Testing and modelling an unglazed photovoltaic thermal collector for application in Sichuan Basin," *Appl. Energy*, vol. 242, pp. 931–941,2019.

[12] F. Yazdanifard, M. Ameri, and E. Ebrahimnia-Bajestan, "Performance of nanofluid-based photovoltaic/thermal systems: A review," *Renew. Sustain. Energy Rev.*, vol. 76, pp. 323–352, 2017.

[13] N. S. B. Rukman, A. Fudholi, N. F. M. Razali, M. H. Ruslan, and K. Sopian, "Energy and exergy analyses of photovoltaic-thermal (PV/T) system with TiO2/water nanofluid flow," in *IOP Conference Series: Earth and Environmental Science*, 2019, vol. 268, no. 1, p. 12075.

[14] A. H. A. Al-Waeli, M. T. Chaichan, H. A. Kazem, K. Sopian, and J. Safaei, "Numerical study on the effect of operating nanofluids of photovoltaic thermal system (PV/T) on the convective heat transfer," *Case Stud. Therm. Eng.*, vol. 12, pp. 405–413, 2018.

[15] A. M. Hussein, R. A. Bakar, K. Kadirgama, and K. V Sharma, "Experimental measurement of nanofluids thermal properties," *Int. J. Automot. Mech. Eng.*, vol. 7, p. 850, 2013.

[16] Z. Qiu, X. Zhao, P. Li, X. Zhang, S. Ali, and J. Tan, "Theoretical investigation of the

energy performance of a novel MPCM (Microencapsulated Phase Change Material) slurry based PV/T module," *Energy*, vol. 87, pp. 686–698, 2015.
[17] M. Firoozzadeh, A. H. Shiravi, M. Lotfi, S. Aidarova, and A. Sharipova, "Optimum concentration of carbon black aqueous nanofluid as coolant of photovoltaic modules: A case study," *Energy*, vol. 225, 2021, doi: 10.1016/j.energy.2021.120219.
[18] Y. Demirel, "Thermodynamic analysis," *Arab. J. Sci. Eng.*, vol. 38, no. 2, pp. 221–249, 2013.
[19] S. R. Maadi, A. Kolahan, M. Passandideh-Fard, M. Sardarabadi, and R. Moloudi, "Characterization of PVT systems equipped with nanofluids-based collector from entropy generation," *Energy Convers. Manag.*, vol. 150, no. August, pp. 515–531, 2017, doi: 10.1016/j.enconman.2017.08.039.
[20] O. R. Alomar and O. M. Ali, "Energy and exergy analysis of hybrid photovoltaic thermal solar system under climatic condition of North Iraq," *Case Stud. Therm. Eng.*, vol. 28, no. May, p. 101429, 2021, doi: 10.1016/j.csite.2021.101429.
[21] A. Fudholi *et al.*, "Energy and exergy analyses of photovoltaic thermal collector with∇-groove," *Sol. Energy*, vol. 159, pp. 742–750, 2018.
[22] M. Sardarabadi, M. Hosseinzadeh, A. Kazemian, and M. Passandideh-Fard, "Experimental investigation of the effects of using metal-oxides/water nanofluids on a photovoltaic thermal system (PVT) from energy and exergy viewpoints," *Energy*, vol. 138, pp. 682–695, 2017, doi: 10.1016/j.energy.2017.07.046.
[23] A. Farzanehnia and M. Sardarabadi, "Exergy in photovoltaic/thermal nanofluid-based collector systems," in *Exergy and Its Application-Toward Green Energy Production and Sustainable Environment*, IntechOpen, 2019.
[24] B. C. Pak and Y. I. Cho, "Hydrodynamic and heat transfer study of dispersed fluids with submicron metallic oxide particles," *Exp. Heat Transf. an Int. J.*, vol. 11, no. 2, pp. 151–170, 1998.
[25] W. Yu and S. U. S. Choi, "The role of interfacial layers in the enhanced thermal conductivity of nanofluids: a renovated Maxwell model," *J. nanoparticle Res.*, vol. 5, no. 1, pp. 167–171, 2003.
[26] Y. Xuan and W. Roetzel, "Conceptions for heat transfer correlation of nanofluids," *Int. J. Heat Mass Transf.*, vol. 43, no. 19, pp. 3701–3707, 2000.
[27] H. C. Brinkman, "The viscosity of concentrated suspensions and solutions," *J. Chem. Phys.*, vol. 20, no. 4, p. 571, 1952.
[28] F. Abbas *et al.*, "Towards convective heat transfer optimization in aluminum tube automotive radiators: Potential assessment of novel Fe2O3-TiO2/water hybrid nanofluid," *J. Taiwan Inst. Chem. Eng.*, vol. 124, pp. 424–436, 2021.
[29] K. S. Hanumanth Ramji, J. Vinoth Kumar, and A. Amar Karthik, "Experimental Investigation of Automobile radiator using Tungsten trioxide Nano-fluid," *IOP Conf. Ser. Mater. Sci. Eng.*, vol. 995, no. 1, 2020, doi: 10.1088/1757-899X/995/1/012017.
[30] A. H. A. Al-Waeli, M. T. Chaichan, H. A. Kazem, and K. Sopian, "Comparative study to use nano-(Al2O3, CuO, and SiC) with water to enhance photovoltaic thermal PV/T collectors," *Energy Convers. Manag.*, vol. 148, pp. 963–973, 2017.
[31] M. Faizal, R. Saidur, S. Mekhilef, and M. A. Alim, "Energy, economic and environmental analysis of metal oxides nanofluid for flat-plate solar collector," *Energy Convers. Manag.*, vol. 76, pp. 162–168, 2013.